Int J Clin Exp Pathol 2015;8(9):10671-10679
www.ijcep.com /ISSN:1936-2625/IJCEP0012796

Original Article

Changes of ferrous iron and its transporters after intracerebral hemorrhage in rats

Gaiqing Wang[1*], Anwen Shao[2*], Weimin Hu[1], Fang Xue[1], Hongping Zhao[3], Xiaojie Jin[4], Guanglai Li[1], Zhitang Sun[1], Li Wang[1]

[1]Department of Neurology, The Second Hospital, Shanxi Medical University, 382 Wuyi Avenue, Taiyuan 030001, Shanxi, China; [2]Department of Neurosurgery, Second Affiliated Hospital, School of Medicine, Zhejiang University, 88 Jiefang Road, Hangzhou 310009, Zhejiang, China; [3]Department of Neurology, Shanxi Large Hospital, Taiyuan 030000, Shanxi,China; [4]Department of Neurology, Tianjin First Center Hospital, Tianjin 300192, China. [*]Equal contributors.

Received July 12, 2015; Accepted August 22, 2015; Epub September 1, 2015; Published September 15, 2015

Abstract: Objective: Ferrous iron is a major source inducing oxidative stress after intracerebral hemorrhage (ICH). Divalent metal transporter1 (DMT1) is the important and well-known plasma membrane transport protein which was proved to be involved in the transport of free ferrous iron in mammals. Ferroportin 1 (FPN1) is the unique exporter of ferrous iron from mammalian cells. The role of DMT1 and FPN1 in brain after ICH is still not elucidated. Therefore, we measure the expression of DMT1 and FPN1, to explore the correlations between ferrous iron and its specific transporters after ICH. Methods: Ninety-six Sprague-Dawley rats received intra-striatal infusions of 0.5 U type IV collagenase to establish ICH model. Ferrous iron content in brain was determined using Turnbull's method. DMT1 and FPN1 expression were examined by immunohistochemical staining and Real-Time quantitative polymerase chain reaction (RT-PCR). With the use of confocal laser microscopy, we determined the colocalization of DMT1 and FPN1 at 1, 3, 7 and 14 days after ICH. Results: Ferrous iron deposition was shown in the perihematomal zone as early as 1 day after ICH; it reached a peak after 7 days and was not elevated within 14 days following ICH. The expression of the DMT1 upregulated and reached to peak at day 7 after ICH. FPN1 reached a plateau at 3 days post-ICH. Expression levels of DMT1 and FPN1 were in parallel with ferrous iron deposition. There was a positive correlation between FPN1 and DMT1. DMT1 mainly localized in the cytoplasm of glias and neurons. FPN1 were mostly distributed on the membrane of endothelial cells and glias. Confocal microscope showed that DMT1 colocalized with FPN1. Conclusions: DMT1 and FPN1 are positively influenced by ferrous iron status in brain after ICH. DMT1 and FPN1 attenuate iron overload after ICH via increasing transmembrane iron export.

Keywords: Ferrous iron, divalent metal transporter1, ferroportin1, intracerebral hemorrhage

Introduction

Excess ferrous iron is deemed to be a major source of oxidative stress due to the production of reactive oxygen species (ROS) through Fenton reaction. The reaction involves the process of inducing the ferrous iron and hydrogen peroxide into a toxic hydroxide ion and a hydroxyl free radical, with the concurrent oxidation of ferrous iron to ferric iron. The ability of the ferrous iron to generate ROS and hydroxyl radicals initiates lipid peroxidation as well as direct DNA damage [1]. Many previous studies revealed the detrimental role of massive iron releasing into the brain after intracerebral hemorrhage (ICH) [2-4], however, there have been few studies focusing on the regulation of iron after ICH. Divalent metal transporter1 (DMT1) is the important known plasma membrane transport protein which was proved to be associated with the transport of free ferrous iron in mammals [5]. Previous studies have demonstrated the importance of the iron transporter DMT1 in iron homeostasis [6, 7]. DMT1 may act as the transporter for free ferrous iron at the blood-cerebrospinal fluid barrier and regulated by the feedback of the iron storage in body [1, 8, 9].

Ferroportin1 (FPN1) is a newly discovered transmembrane iron export protein. It plays a key

role in Fe^{2+} transport across the basal membrane of enterocytes and iron export during erythrocyte-iron recycling by macrophages [10]. Recent findings suggest that FPN1 is expressed in brain and might play a role in ferrous iron export of nerve cells [11]. Some previous researchers explored the relationship between ferrous iron tranporters and iron regulation [12, 13], however, the crosstalk of ferrous iron tranporters and iron in ICH-induced iron overload is still unclear.

Based on the evidence mentioned above, we hypothesis that iron fluxes in brain cells can be determined by the activity of import and export transporters. To elucidate the underlying mechanisms of ferrous *iron regulation after ICH*, we explored the colocalization of DMT1 and FPN1, detected the associated transporters response to the ferrous iron status, which my help to clarify the possible iron transport way in ICH condition.

Materials and methods

Animal preparation

The protocols for these animal studies were approved by the Committee of Shanxi medical University for the Use and Care of Animals. A total of 96 adult male Sprague-Dawley rats (Animal Laboratories of Shanxi medical University) weighing 250 to 300 g were used in the study. These rats were randomly divided into 2 groups. Group A were 48 control rats (received a 2.5 μL intracerebral infusion of saline); Group B were 48 ICH rats (received a 2.5 μL saline plus 0.5 U collagenase IV). At 1, 3, 7, and 14 days post-ICH, the rats were killed by an overdose of chloral hydrate (400 mg/kg, i.p.).

The experiment consists of 4 parts. In Part 1, we examined the ferrous iron deposition using Turnbull's staining; In part 2, DMT1 and FPN1 expression around hematoma were analyzed by immunohistochemical staining; In part 3, confocal microscopy was used to determine the colocalization of DMT1 and FPN1; In part 4, RT-PCR was used to quantify the expression of DMT1 and FPN1.

ICH model

The rats were anesthetized with an intraperitoneal injection of hydrated chloric aldehyde (300-350 mg/kg) and were allowed free access to food and water before the procedure. The rats were placed in a stereotactic head frame (Jiangwan type 1 C Instrument, Shanghai, China) after anesthesia, and a 1 mm cranial burr hole was drilled on the right coronal suture 2.3 mm lateral to midline. Then, 2.5 μL saline including 0.5 U collagenase IV was infused into the right caudate slowly (coordinates: 0.5 mm anterior, 5.8 mm ventral, and 2.3 mm lateral to the bregma) using 5 μL flat-headed microsyringe (Hamilton 600, Switzerland). In sham-operated animals, 2.5 μL saline was infused. Then the needle was withdrawn, the bur hole was filled with bone wax, and the skin incision was sutured.

Brain section preparation

Rats were anesthetized and underwent intracardiac perfusion with 4% paraformaldehyde in 0.1 mol/L (pH 7.4) phosphate-buffered saline. The brains were removed immediately and a 5-mm-thick coronal brain section containing the injection site was isolated. The brain section were kept in 4% paraformaldehyde at 4°C, then placed in serial dehydrating, embodying in wax and 5-μm-thick coronal slices were obtained. The sections were dewaxed in xylene and rehydrated in a graded series of ethanol baths.

Turnbull's method for ferrous iron staining

① Incubate in Turnbull's staining solution (1:1, Reagent F 100 μL and Reagent G 100 μL) for 60 min and rinse in distilled water; ② Place in cleaning solution 50ml (Reagent E) for 2 min then wash in distilled water; ③ Place in blockading solution (Reagent H) for 20 min and remove the solution, then repeat step ②; ④ Incubate in dark place with coloration solution 200 μL (Reagent I) for 20 min rinse in distilled water; ⑤ Incubate in dark place with coloration working solution 200 μL (Reagent I 200 μL mixed with Reagent J 1.8 ml) for 15 min and rinse in distilled water, then repeat step ②; ⑥ Dehydrate in 95% alcohol, absolute alcohol and clear in xylene, two changes each; ⑦ Mount with permount. Two images were taken from the caudate just next to the cavity. Area measurements were performed on two areas in each of six rat brain sections from group A and B. Brain iron positive area were assayed by colorful medical imaging instruments (image-pro plus 6.0, OLYMPUSBX60, German).

Immunohistochemical staining for DMT1 and FPN1

Before labeling, endogenous peroxidase activity in deparaffinized sections was blocked with 3% H_2O_2. Sections were then incubated in PBS for 30 min at room temperature. After wet heat-induced epitope retrieval, the sections were incubated with 5% bovine serum albumin in PBS for 20 min. Primary rabbit anti-mouse DMT1 (1:200 dilution, Lanji Biotech Corporation, Shanghai, China) and mouse anti-rat FPN1 (1:200 dilution, Boaosen Biotech Corporation, Shanghai, China) were added respectively and incubated overnight at 4°C in a humidified box. After washed 3 times with PBS for 10 min, the brain sections were incubated with biotinylated goat anti-rabbit and goat anti-mouse secondary antibodies (Boshide Bioengineering Corporation, Wuhan, China) for 35 min at 37°C. After washing, the sections were treated with streptavidin- biotin complex (Boshide Bioengineering Corporation) for 20 min at 37°C. The sections were then washed 3 times with PBS for 5 min and the staining reaction was carried out using 3, 3'-diaminobenzidine tetrahydrochloride (DAB) as the chromogen. Negative controls included incubation with PBS without the primary antibody. The sections were dehydrated in ethanol, cleared in xylene, and cover-slipped. Finally, slices were photographed with colorful medical imaging instruments (image-pro plus 6.0, OLYMPUSBX60, German). The same areas were selected for imaging in corpus striatum. The photographs were analyzed with the Image-Pro Plus software. Two areas were selected, the number of positively stained cells was determined in each section, and counts were determined from three sections per animal.

Immunofluorescence for DMT1 and FPN1 with laser confocal microscopy

Immunofluorescence detection of DMT1 and FPN1 in brain was performed by using both primary antibodies which were added at the same time, the specific steps described in detail as mentioned above. The primary antibody was removed, and the sections were washed in high-salt PBS (2.8% wt/vol NaCl), followed by two times wash with PBS. The slides were then incubated for 1 h at room temperature with the appropriate secondary antibodies, which were goat anti-rabbit IgG conjugated to FITC and goat anti-mouse IgG conjugated to Cy3. All secondary antibodies were applied simultaneously. After incubation with the secondary antibodies, all sections were washed twice for 5 min in high-salt PBS, followed by two times wash in PBS, and mounted with Vectashield (Vector Labs, Burlingame, CA). Omission of primary antibody during development resulted in no detectable signals. Immunostaining was observed and photographed using an Olympus Fluoview FV1000 confocal laser scanning microscope (Olympus America Inc, USA).

Real-time quantitative polymerase chain reaction (RT-PCR)

Total RNA was extracted from brain tissues stored at -80°C by use of TRIzol Reagent (Sigma-Aldrich, USA) in accordance with the manufacturer's instructions. Complementary DNA was reverse transcribed using a 2-step RT-PCR kit (Takara Bio, China). RT-PCR analysis was performed using ABI7300System SDS RQ Study Software (Life Technologies, USA) with the SYBR green RT-PCR Kit (Takara Bio, China). A 20-μL total reaction mixture volume was used in the PCR; this contained 8μL of diluted complementary DNA reaction products, 10 μL of SYBR green PCR Master Mix, and 2 μL of forward and reverse primers. Reaction conditions were as follows: initial denaturation at 95°C for 2 minutes, 40 cycles of denaturation at 95°C for 30 seconds, and annealing and elongation at 60°C for 45 seconds. Reverse transcription was performed in triplicate. To standardize DMT1 and FPN1 mRNA concentrations, transcript levels of the housekeeping gene β-actin were determined in parallel for each sample. Final results were expressed as the copy ratio of β-actin transcripts. The amount of target was calculated by the $2^{-\Delta\Delta Ct}$ method [14].

Statistical analysis

All data in this study are presented as the mean ± standard division (SD). SPSS 13.0 was used for data analysis. Normal distribution test, Homogeneity test of variance, Dunnet T3 multiple comparison test, Student's *t* -test and Pearson's test were carried out for the data. Significance levels were measured at a probability value less than 0.05.

Results

Histochemical assessment for iron

Based on Turnbull's iron staining method, iron positive staining appeared as a brown deposit in the perihematomal zone as early as the 1 day

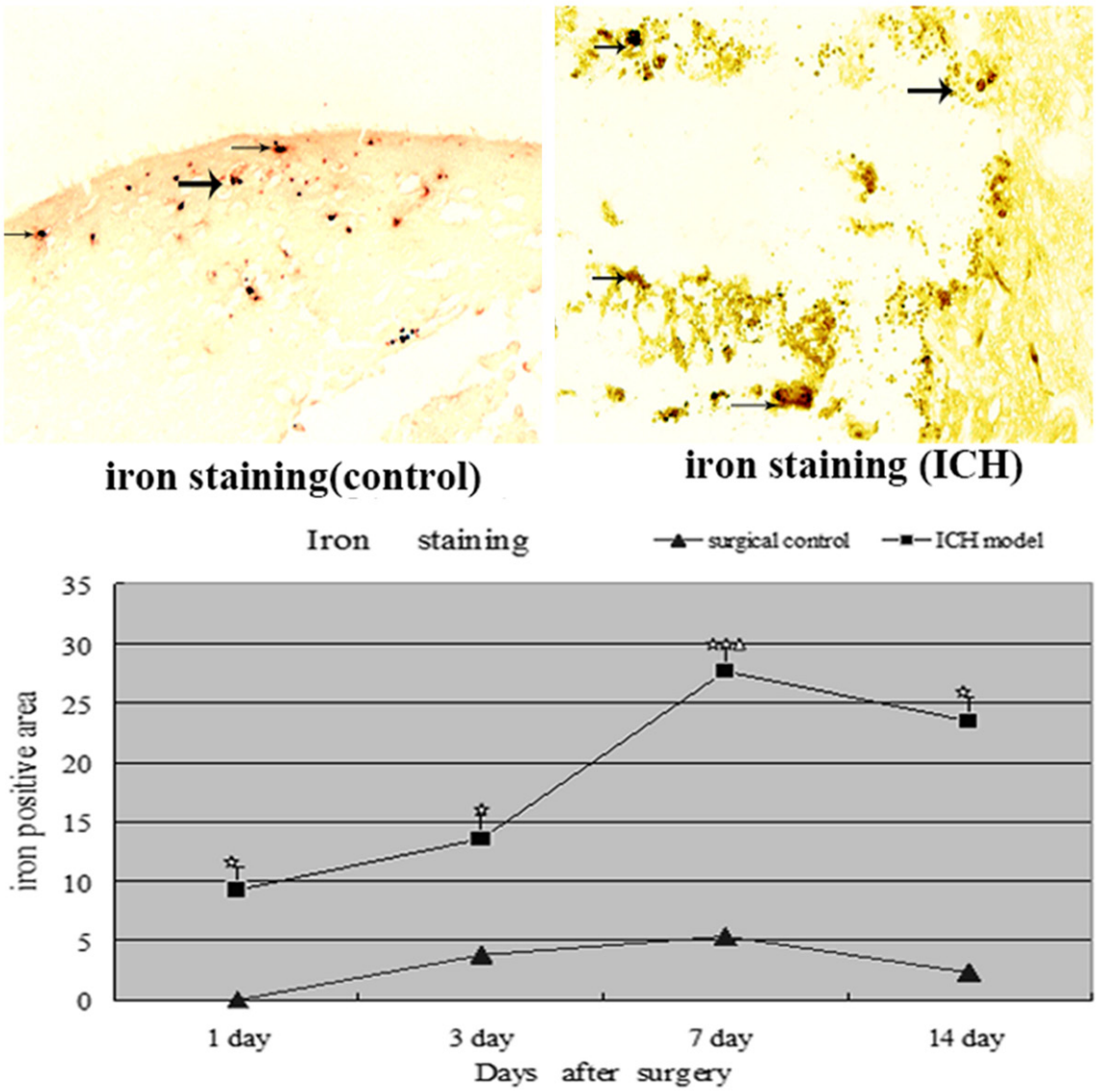

Figure 1. Photomicrograph of perihematomal tissue showed Turnbull's staining for ferrous iron deposit in a rat at day 7 after surgery. Results of the ferrous iron-positive area in surgical controls ▲ and ICH models ■. $^{☆}P < 0.05$, $^{☆☆}P < 0.01$ vs. controls; $^{\Delta}P < 0.05$ vs. former point by Dunnett's T3 multiple comparison tests.

post-ICH and reached a plateau at 7 days (27.67 ± 5.89 in the ICH group vs 5.41 ± 0.53 in control group, $P < 0.01$), iron deposition remained at high levels for at least 14 days (23.40 ± 6.18 in the ICH group vs 2.33 ± 0.42 in control group, $P < 0.05$). A few iron positive staining cells were observed around needle passage after 3 days in surgical control rats (**Figure 1**).

DMT1 expression and assay

As shown in **Figure 2**, DMT1 were found predominantly in the cytoplasm of neurons, some were in glia and a few were in endothelial cells. There was an increased expression of DMT1 at each time point around hematoma in brain. DMT1 reached a plateau at day 7 after ICH.

The presence of FPN1 by immunohistochemistry

In **Figure 3**, FPN1 expression was mainly at membrane of endothelial cells which is consistent with its role for iron exportation from brain, the other located at glia. Similar to DMT1, all animals showed that FPN1 expression was significantly increased in ICH group compared to sham-operated animals. FPN1 reached a plateau at day 3 post-ICH.

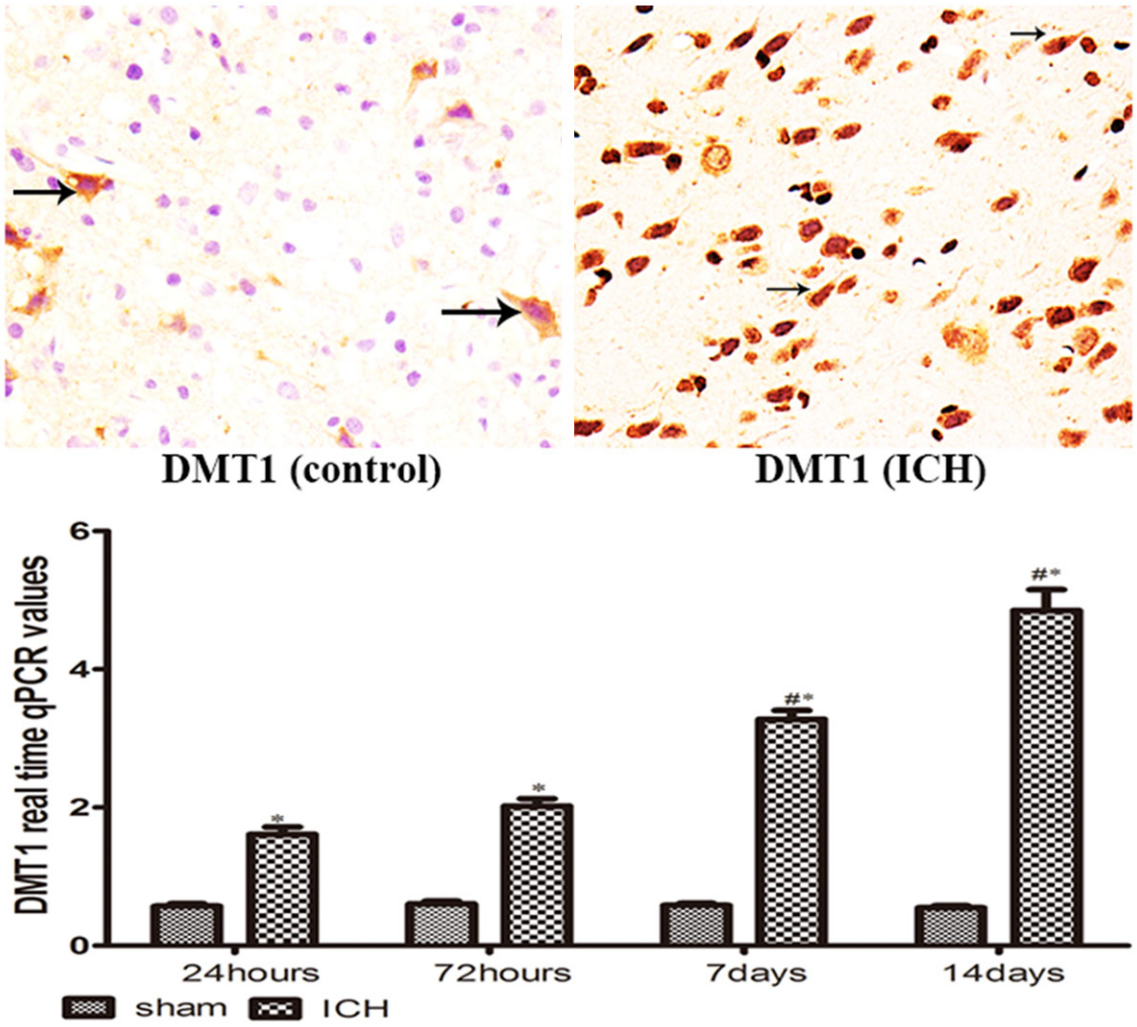

Figure 2. DMT-1 immuno-positive cells (brown) were shown at day 7 after operation; $^{*}P < 0.05$ vs. controls, $^{\#}P < 0.05$ vs. former point by Dunn T3 multiple comparison test.

Colocalization of DMT1 and FPN1 in brain after ICH

The colocalization of DMT1 and FPN1 was investigated in brain by double-labeled immunofluorescence. Analysis by confocal microscopy indicated that in most glias and endothelial cells DMT1 (green) produced a punctate intracellular staining consistent with localization in endosomes (**Figure 4A**), membrane and cytoplasmic staining was observed in the similar and adjacent cells with the anti-FPN1 antiserum (red, **Figure 4B**) at day 7 after ICH. Superimposition of the images (**Figure 4C**) clearly showed overlapping staining of the 2 signals. Surprisingly, in contrast to data on 7 day, DMT1 colocalized with FPN1 at other days in brain after ICH (**Figure 4D**, **4E**), superimposition shows yellow overlapping staining (**Figure 4F**).

Relationship between iron deposits and the ferrous iron transporters

The levels of ferrous iron accumulation showed positively correlation with DMT1 ($r = 0.338$, $P < 0.01$) and FPN1 ($r = 0.338$, $P < 0.01$). The expression of DMT1 was correlated significantly with FPN1 following ICH ($r = 0.834$, $P < 0.001$).

Discussion

Intracerebral hemorrhage (ICH) is a devastating type of stroke with the highest mortality rate, leading to significant impairment from mechanical trauma and secondary injury. Free iron,

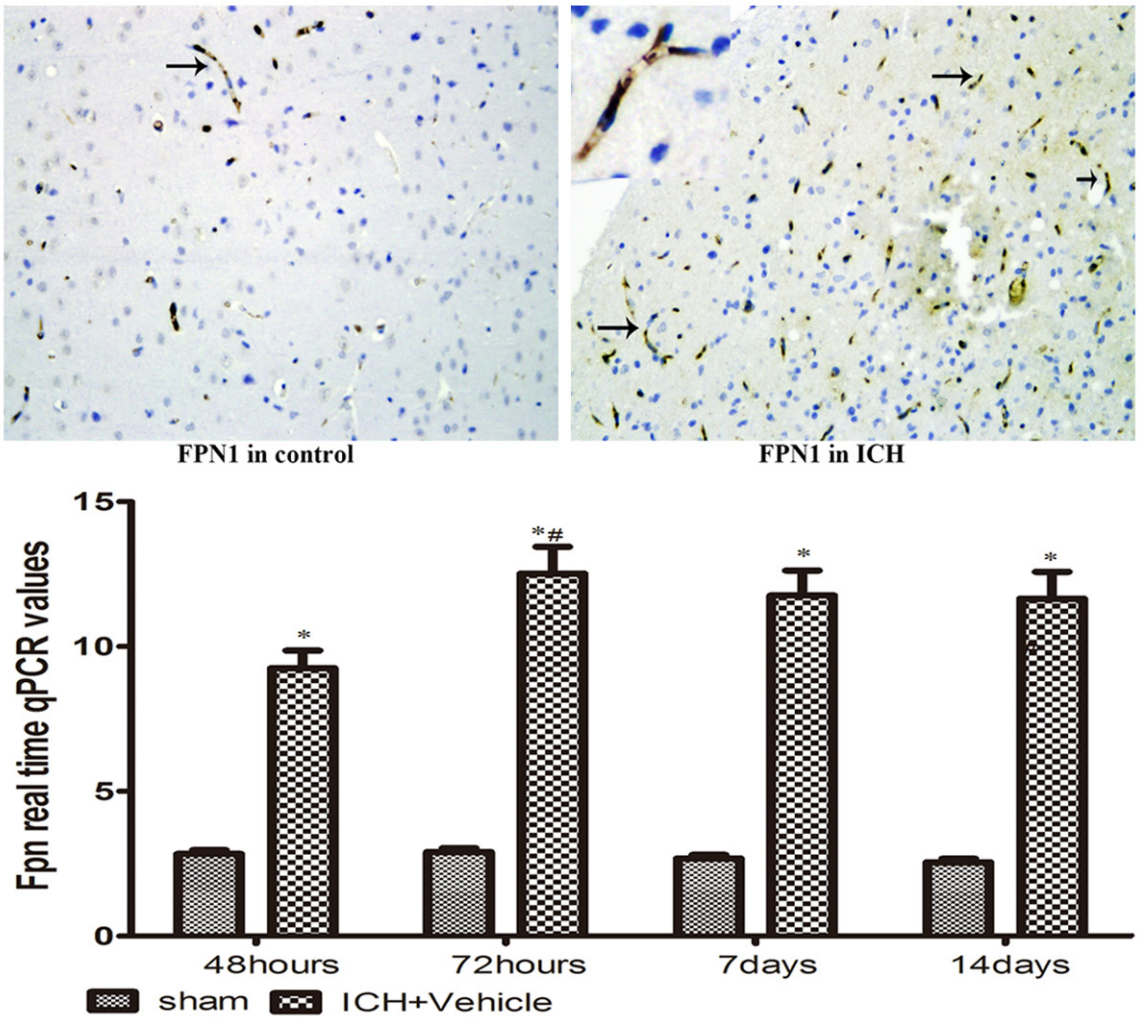

Figure 3. FPN-1 immuno-positive cells (brown) were shown at day 7 after operation; $^{*}P < 0.05$ vs. controls, $^{\#}P < 0.05$ vs. former point by Dunnett's T3 multiple comparison test.

released from lysed erythrocytes, results in free radicals generation which likely contribute to delayed injury [15]. Iron, especially in its ferrous state, has the potential to generate highly cytotoxic hydroxyl radicals via catalyzing the Fenton chemistry [16]. The exact removal process for excess ferrous iron from the brain remains unknown. Therefore, to decrease the risk of ferrous iron-mediated cellular injury, the therapeutic control of excess ferrous iron accumulation in the brain after ICH is required. In this concern, knowledge of the ferrous iron transporters localization and reducing state of iron would be highly useful for the improvement of prognosis after ICH.

The findings in the present study confirm that ferrous iron accumulated in the brain after ICH. Ferrous iron was found around the hematoma as early as the day 1 and reach the peak by the day 7 after ICH as detected by Turnbull's iron staining. This probably reflects the delayed lysis of erythrocytes after ICH [1, 17].

Divalent metal transporter1 (DMT1), the major iron importer, as an integral membrane protein, is the best characterized Fe^{2+} transporter involved in cellular iron uptake in mammals [18]. DMT1 has been detected in every cell type and its structure is highly conserved in evolution with similar proteins expressed in many different organisms [5, 19-20]. In the brain, DMT1 mRNA is consistently found in neurons, astrocytes, cerebral capillary endothelial cells that constitute the blood-brain barrier and the choroid plexus epithelial cells that comprise the

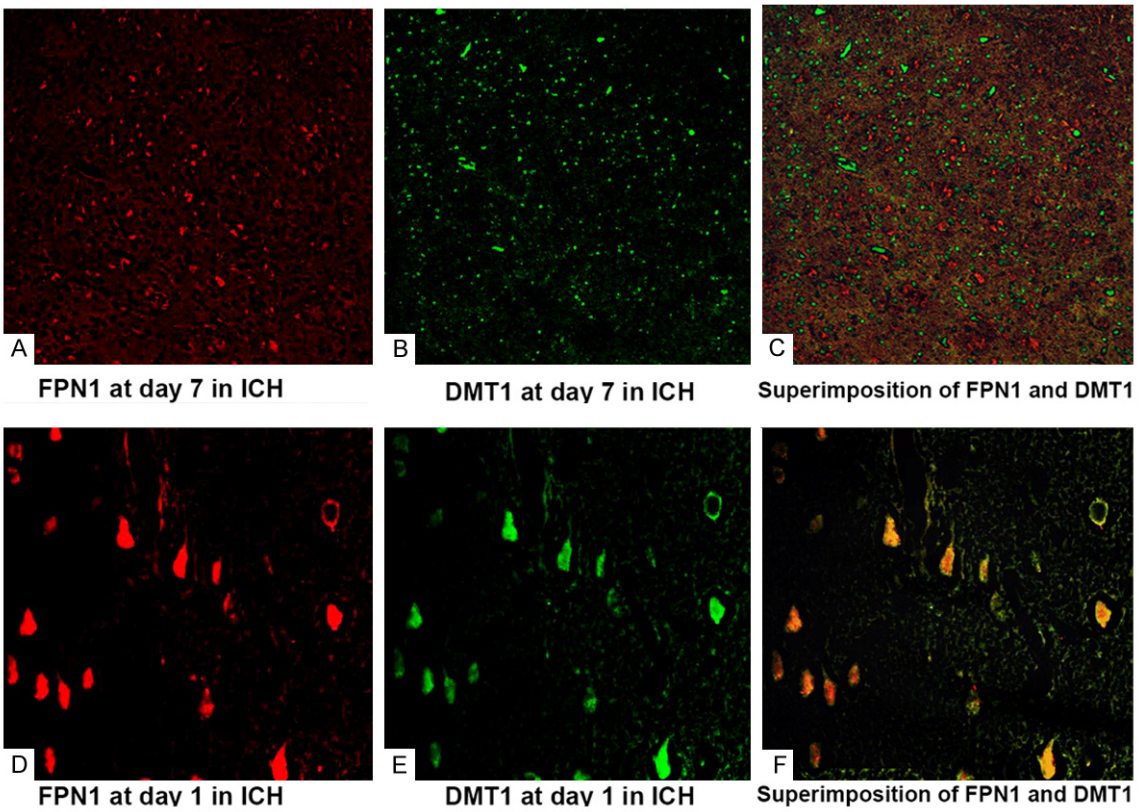

Figure 4. Localization of DMT1 (A. 7 day after ICH; D. 1 day after ICH; Green fluorescence) and FPN1 (B. 7 day after ICH; E. 1 day after ICH; Red fluorescence); DMT1 colocalized with FPN1 (C. Superimposition at day 7 after ICH; F. Superimposition at day 1 after ICH, Yellow fluorescence) by double-labeled immunofluorescence.

blood-cerebrospinal fluid barrier and presents at moderate levels in the substantia nigra [12, 19, 21, 22]. DMT1 only transports iron of the ferrous form across the plasma and/or endosomal membrane. Studies on brain barriers have also suggested that iron can pass across the BBB and cerebrospinal fluid barrier into the central nervous system via a non-Tf-mediated transport [19, 23, 24]. The cellular localization and functional characterization of DMT1 suggest that it might participate in physiological brain iron homeostasis and transport [12, 22, 25]. Wang XS et al have reported that DMT1 expression is closely linked to iron levels, dysregulation of DMT1 seems to take part in some neurodegenerative disorders [12], and provide more support for a key role that DMT1 plays in iron overload in the degenerating hippocampus [26, 27]. Upregulation of DMT1 may result in excessive iron accumulation, and, finally, cause neurodegeneration in the region of the brain. Until now there was no research about the change of DMT1 expression when iron overload happens in brain after ICH. Our study showed that DMT1 was increased in all ICH rats and reached maximum at day 7 compared to the operated control rats. A positive relationship was observed between ferrous iron and DMT1. Given the accumulation of iron, the increase in the expression of the iron importer DMT1 was unexpected. These data also suggest that DMT1 may play an important role in iron trafficking in brain after ICH.

FPN1, as well as DMT1, are highly involved in iron transport. Studies demonstrate that neurons express ferroportin which could reflect a mechanism for iron export [28]. Cellular iron efflux involves ferroportin, the unique known iron exporter. Ferroportin is found in most cell types, and export iron into plasma [29]. Although it has not been proven directly, FPN appears to transport ferrous iron. Similar to DMT1, our experiment also demonstrated that FPN1 upregulated after ICH and reached a peak at day 3 compared to the surgical control

rats. A positive relationship was observed between ferrous iron and FPN1. The similar correlation was existed between FPN1 and DMT1. Our findings suggest that the role of FPN1 in ferrous iron export after ICH and a possible ambivalent role of DMT1.

In spite of a consistent expression of FPN1 and DMT1, there is no real information on whether the both iron transporters are capable of exporting the accumulated ferrous iron after ICH. Our staining showed that DMT1 was found predominantly localized in nucleus and cytoplasm of glial cells and neurons (**Figure 2**) and FPN1 were mostly distributed on the membrane in endothelial cells (**Figure 3**). Meanwhile our colocalization studies with laser scanning confocal microscopy provided support for the both protein interactions. Superimposition images (**Figure 4C**) showed overlapping staining of the two ferrous iron transporters at day 7 in ICH. These results indicated that DMT1 was located in cytoplasm of glias while FPN1 was located on the endothelia and glia cell surfaces. Unpredictably, DMT1 and FPN1 were colocalized in neurons at day 1 in brain after ICH (**Figure 4D**, **4E**). Export of iron from astrocytes is mediated by ferroportin. This process has been discussed to be important for the supply of iron to other brain cell types such as neurons [30, 31]. Ferroportin-mediated iron export from astrocytes requires ferrous iron as substrate [30]. DMT1 is major the transporter for ferrous iron entrance into mammalian cells, but it also plays a similar major role in export of iron from the endosome during the transferrin cycle [18, 32, 33]. DMT1 is known to be trafficked throughout the cell via the endosomal pathway [34]. DMT1 on the cell surface may play a role in iron influx into cells, and DMT1 on the endosomal membrane has been shown to be required for the transport of iron from the endosome into the cytosol [34, 35]. Therefore, the increase in DMT1 expression after ICH do not show evidence of its role for iron accumulation, suggests that these cells are trying to increase iron exit from endosome to cytoplasm by upregulating DMT1. Moreover our results also illustrated that neurons are capable of exporting iron to the cellular exterior.

In conclusion, DMT1 and FPN1 were positively regulated by ferrous iron status in brain after ICH, DMT1 assisted in transmembrane iron export along with FPN1 while iron overload after ICH. More knowledge about these processes in the brain will be needed and well documented.

Acknowledgements

This study was supported by a grant from Shanxi provincial Science and Technology Agency (basic research project number: 2014011041-5) and Shanxi provincial Hygiene Department (Item number: 201301010).

Disclosure of conflict of interest

None.

Address correspondence to: Dr. Gaiqing Wang, Department of Neurology, The Second Hospital, Shanxi Medical University, 382 Wuyi Avenue, Taiyuan 030001, Shan Xi, China. Tel: + 86 13466838438; E-mail: wanggq08@126.com

References

[1] Popescu BF, Nichol H. Mapping brain metals to evaluate therapies for neurodegenerative disease. CNS Neurosci Ther 2011; 17: 256-268.

[2] Wu J, Hua Y, Keep RF, Nakamura T, Hoff JT, Xi G. Iron and iron-handling proteins in the brain after intracerebral hemorrhage. Stroke 2003; 34: 2964-2969.

[3] Huang F, Xi G, Keep RF, Hua Y, Nemoianu A, Hoff JT. Brain edema after experimental intracerebral hemorrhage: role of hemoglobin degradation products. J Neurosurg 2002; 96: 287-293.

[4] Wu J, Hua Y, Keep RF, Schallert T, Hoff JT, Xi G. Oxidative brain injury from extravasated erythrocytes after intracerebral hemorrhage. Brain Res 2002, 95: 45-52.

[5] Mims MP, Prchal JT. Divalent metal transporter 1. Hematology 2005; 10: 339-345.

[6] Anderson GJ, Frazer DM, McKie AT, Wilkins SJ, Vulpe CD. The expression and regulation of the iron transport molecules hephaestin and IREG1: implications for the control of iron export from the small intestine. Cell Biochem Biophys 2002; 36: 137-146.

[7] Wu LJ, Leenders AG, Cooperman S, Meyron-Holtz E, Smith S, Land W, Tsai RY, Berger UV, Sheng ZH, Rouault TA. Expression of the iron transporter ferroportin in synaptic vesicles and the blood-brain barrier. Brain Research 2004; 1001: 108-117.

[8] Qian ZM, Shen X. Brain iron transport and neurodegeneration. Trends Mol Med 2001; 7: 103-108.

[9] Canonne-Hergaux F, Fleming MD, Levy JE, Gauthier S, Ralph T, Picard V, Andrews NC, Gros P. The Nramp2/DMT1 iron transporter is

induced in the duodenum of microcytic anemia mk mice but is not properly targeted to the intestinal brush border. Blood 2000; 96: 3964-3970.
[10] Jiang DH, Ke Y, Cheng YZ, Ho KP, Qian ZM. Distribution of ferroportin1 protein in different regions of developing rat brain. Dev Neurdsci 2002; 24: 94-98.
[11] Ding H, Yan CZ, Shi H, Zhao YS, Chang SY, Yu P, Wu WS, Zhao CY, Chang YZ, Duan XL. Hepcidin is involved in iron regulation in the ischemic brain. PLoS One 2011; 6: e25324.
[12] Gunshin H, Mackenzie B, Berger UV, Gunshin Y, Romero MF, Boron WF, Nussberger S, Gollan JL, Hediger MA. Cloning and characterization of a mammalian proton-coupled metal-ion transporter. Nature 1997; 388: 482-488.
[13] Fleming MD, Romano MA, Su MA, Garrick LM, Garrick MD, Andrews NC. Nramp2 is mutated in the anemic Belgrade (b) rat: evidence of a role for Nramp2 in endosomal iron transport. Proc Natl Acad Sci U S A 1998; 95: 1148-1153.
[14] Livak KJ, Schmittgen TD. Analysis of relative gene expression data using real-time quantitative PCR and the 2 (-Delta DeltaC (T)) Method. Methods 2001; 25: 402-408.
[15] Caliaperumal J, Ma Y, Colbourne F. Intra-parenchymal ferrous iron infusion causes neuronal atrophy, cell death and progressive tissue loss: implications for intracerebral hemorrhage. Exp Neurol 2012; 237: 363-369.
[16] Meguro R, Asano Y, Odagiri S, Li C, Shoumura K. Cellular and subcellular localizations of nonheme ferric and ferrous iron in the rat brain: a light and electron microscopic study by the perfusion-Perls and -Turnbull methods. Arch Histol Cytol 2008; 71: 205-222.
[17] Xi G, Keep RF, Hoff JT. Erythrocytes and delayed brain edema formation following intracerebral hemorrhage in rats. J Neurosurg 1998; 89: 991-996.
[18] Pelizzoni I, Zacchetti D, Smith CP, Grohovaz F, Codazzi F. Expression of divalent metal transporter 1 in primary hippocampal neurons: reconsidering its role in non-transferrin-bound iron influx. J Neurolhem 2012; 120: 269-278.
[19] Vidal S, Belouchi AM, Cellier M, Beatty B, Gros P. Cloning and characterization of a second human NRAMP gene on chromosome 12q13. Mamm Genome 1995; 6: 224-230.
[20] Georgieff MK, Wobken JK, Welle J, Beatty B, Gros P. Identification and localization of divalent metal transporter-1 (DMT-1) in term human placenta. Placenta 2000; 21: 799-804.
[21] Siddappa AJ, Rao RB, Wobken JD, Casperson K, Leibold EA, Connor JR, Georgieff MK. Iron deficiency alters iron regulatory protein and iron transport protein expression in the perinatal rat brain. Pediatr Res 2003; 53: 800-807.
[22] Ke Y, Chang YZ, Duan XL, Du JR, Zhu L, Wang K, Yang XD, Ho KP, Qian ZM. Age-dependent and iron-independent expression of two mRNA isoforms of divalent metal transporter 1 in rat brain. Neurobiol Aging 2005; 26: 739-748.
[23] Bradbury MW. Transport of iron in the blood-brain-cerebrospinal fluid system. J Neurochem 1997; 69: 443-454.
[24] Moos T, Morgan EH. The significance of the mutated divalent metal transporter (DMT1) on iron transport into the Belgrade rat brain. J Neurochem 2004; 88: 233-245.
[25] Williams K, Wilson MA, Bressler J. Regulation and developmental expression of the divalent metal-ion transporter in the rat brain. Cell Mol Biol (Noisy-le-grand) 2000; 46: 563-571.
[26] Song N, Jiang H, Wang J, Xie JX. Divalent metal transporter 1 up-regulation is involved in the 6-hydroxydopamine-induced ferrous iron influx. J Neurosci Res 2007; 85: 3118-3126.
[27] Ke Y, Ming Qian Z. Iron misregulation in the brain: a primary cause of neurodegenerative disorders. Lancet Neurol 2003; 2: 246-253.
[28] Boserup MW, Lichota J, Haile D, Moos T. Heterogenous distribution of ferroportin-containing neurons in mouse brain. BIometals 2011; 24: 357-375.
[29] Graham RM, Chua AC, Herbison CE, Olynyk JK, Trinder D. Liver iron transport. World J Gastroenterol 2007; 13: 4725-4736.
[30] Hohnholt MC, Dringen R. Uptake and metabolism of iron and iron oxide nanoparticles in brain astrocytes. Biochem Soc Trans 2013; 41: 1588-1592.
[31] Dringen R, Bishop GM, Koeppe M, Dang TN, Robinson SR. The pivotal role of astrocytes in the metabolism of iron in the brain. Neurochem Res 2007; 32: 1884-1890.
[32] Garrick MD, Zhao L, Roth JA, Jiang H, Feng J, Foot NJ, Dalton H, Kumar S, Garrick LM. Isoform specific regulation of divalent metal (ion) transporter (DMT1) by proteasomal degradation. Biometals 2012; 25: 787-793.
[33] Garrick M. Human iron transporters. Genes & Nutrition 2011; 6: 45-54.
[34] Foot NJ, Dalton HE, Shearwin-Whyatt LM, Dorstyn L, Tan SS, Yang B, Kumar S. Regulation of the divalent metal ion transporter DMT1 and iron homeostasis by a ubiquitin- dependent mechanism involving Ndfips and WWP2. Blood 2008; 112: 4268-4275.
[35] Skjørringe T, Møller LB, Moos T. Impairment of interrelated iron- and copper homeostatic mechanisms in brain contributes to the pathogenesis of neurodegenerative disorders. Front Pharmacol 2012; 3: 169.